Electronic Supplementary Material (ESI) for Chemical Science
This journal is © The Royal Society of Chemistry 2013

Supplementary Information

One-Pot Synthesis of an Inorganic Heterostructure: Uniform Occlusion of Magnetite Nanoparticles within Calcite Single Crystals

Alexander N. Kulak[1], Mona Semsarilar[2], Yi-Yeoun Kim[1], Johannes Ihli[1], Lee A. Fielding,[2] Oscar Cespedes,[3] Steven P. Armes[2] and Fiona C. Meldrum[1]

[1]School of Chemistry, University of Leeds, Woodhouse Lane, Leeds, LS2 9JT, UK.

[2]Dainton Building, Department of Chemistry, University of Sheffield, Brook Hill, Sheffield, Yorkshire, S3 7HF, UK

[3]School of Physics and Astronomy, University of Leeds, Woodhouse Lane, Leeds, LS2 9JT, UK.

Experimental

Calcite single crystal/ magnetite nanoparticle (MNP) composites were prepared by co-precipitation of calcium carbonate with MNPs functionalized with $PMAA_{23}$-$PStSNa_{200}$ stabilizers, and the incorporation efficiency of the MNPs was investigated.

*Materials for Polymer Synthesis***.** All reagents were purchased from Sigma-Aldrich and were used as received unless otherwise stated. 4,4'–azobis-4-cyanopentanoic acid (ACVA) was used as the initiator while 4-cyano-4-(2-phenylethane sulfanylthiocarbonyl) sulfanyl pentanoic acid (PETTC) was synthesized as reported previously.[1]

Synthesis of Poly(methacrylic acid) (PMAA) macro-CTA. A round-bottomed flask was charged with MAA (5.00 g; 58.0 mmol), PETTC (986 mg; 2.10 mmol), ACVA (163 mg, 0.58 mmol) and ethanol (10.0 g). The sealed reaction vessel was purged with nitrogen and placed in a pre-heated oil bath at 70˚C for 3 h. The resulting PMAA macro-CTA (MAA conversion = 90 %; after methylation, M_n =3,550 g mol^{-1}, M_w = 41,000 g mol^{-1}, M_w/M_n = 1.15) was purified using dialysis, first against a 1:1 water: methanol mixture and then against pure deionised water. The polymer was isolated by lyophilisation. A mean DP of 23 was calculated for this macro-CTA using ^{1}H NMR by comparing the integrated signal intensity due to the aromatic protons at 7.2-7.4 ppm with that due to the methacrylic polymer backbone at 0.4-2.5 ppm.

Synthesis of poly(methacrylic acid)-poly(sodium 4-styrenesulfonate) (PMAA-PStSNa) diblock copolymer. StSNa (5.00 g; 24.0 mmol), ACVA (6.80 mg; 0.024 mmol) and $PMAA_{23}$ macro-CTA (0.240 g; 0.120 mmol) were dissolved in water (10.0 g). The reaction mixture was sealed in a round-bottomed flask, purged with nitrogen for 15 min and then placed in a pre-heated oil bath at 70°C for 18 h to produce the desired $PMAA_{23}$-$PStSNa_{200}$ diblock copolymer (StSNa conversion = 100 %).

*Analysis of Polymers***.** Molar mass and molar mass distributions of the block copolymers were measured using size exclusion chromatography (SEC). The experimental set-up comprised two 5 μm (30 cm) mixed C columns and a WellChrom K-2301 refractive index detector operating at 950 ± 30 nm. The eluent used was THF containing 2 v/v % of triethylamine and 0.05 wt/v % of butylhydroxytoluene (BHT) at a flow rate of 1.0 mL min^{-1}. A series of 10 near-monodisperse linear poly(methyl methacrylates) (M_p from 1,280 to 330,000 g mol^{-1}) were purchased from Polymer Labs and were employed as calibration standards with the above refractive index detector. NMR spectra were acquired on a Bruker 250 MHz or 400 MHz spectrometer in D_2O or CD_3OD and all chemical shifts are reported in ppm (δ). TEM studies were conducted using a Philips CM 100 instrument operating at 100 kV, where TEM samples were prepared by placing 5 μL of a dilute aqueous copolymer solution onto a carbon-coated copper grid and drying under ambient conditions. DLS measurements were conducted using a Malvern Instruments Zetasizer Nano series instrument equipped with a 4 mW He-Ne laser operating at 633 nm, an avalanche photodiode detector with high quantum efficiency, and an ALV/LSE-5003 multiple tau digital correlator electronics system. Aqueous electrophoresis measurements were performed on a 0.01 wt% aqueous copolymer solution using the same Malvern Instruments Zetasizer Nano series instrument, where the solution pH was adjusted by the addition of 0.01 M HCl or 0.01 M KOH using an autotitrator.

Chemical Modification of the PMAA$_{23}$ macro-CTA. For size exclusion chromatography analysis, the PMAA$_{23}$ macro-CTA was fully methylated using excess trimethylsilyldiazomethane as reported by Couvreur *et al.*[2] Briefly, PMAA$_{23}$ macro-CTA (50 mg) was dissolved in THF and a yellow solution of trimethylsilyldiazomethane was added dropwise at room temperature. Upon addition, bubbles appeared and the solution became instantaneously colourless. Addition of trimethylsilyldiazomethane was continued until the solution became yellow and stopped bubbling. A small excess of trimethylsilyldiazomethane was then added and the reaction solution was stirred for 6 h at room temperature. Complete methylation was confirmed by ^{1}H NMR analysis.

Synthesis of PMAA$_{23}$-PStSNa$_{200}$ diblock copolymer stabilized magnetite particles (MNP). These particles were prepared following the method described by Armes et al.[3] An aqueous sol of ultrafine magnetite nanoparticles was synthesized by coprecipitation of ferric and ferrous salts in the presence of the PMAA$_{23}$-PStSNa$_{200}$ stabilizer on addition of ammonium hydroxide. In a typical procedure, 200 mg of copolymer stabilizer, 232.2 mg of iron(III) chloride hexahydrate, and 85.8 mg of iron(II) chloride tetrahydrate were dissolved in 3 mL water in a 10 mL flask equipped with a stirrer and rubber septum and this mixture was deoxygenated by purging with dried N$_2$ for at least 30 min. The reaction flask was then immersed in an oil bath set at 80 °C, and after 10 min, 1.0 mL of ammonia solution (28%) was injected by syringe. The solution rapidly became black, indicating the formation of magnetite nanoparticles. The reaction was stirred for 1 h at 80 °C, after which purification of the magnetite sol was achieved by washing with water, followed by two centrifugation cycles (12,000 rpm for 30 min), and redispersal of the sedimented particles was achieved by ultrasonication. The final concentration of the $PMAA_{23}$-$PStSNa_{200}$ copolymer-stabilized magnetite particles were 55.0 mg/mL.

Precipitation of Calcium Carbonate: Calcium carbonate was precipitated using the ammonium carbonate diffusion method in the presence of magnetite nanoparticles (MNP) which were either uncoated, or coated with $PMAA_{23}$-$PStSNa_{200}$.[4] Solutions of $CaCl_2.2H_2O$ (Sigma-Aldrich) with concentrations ranging from 3 mM to 20 mM were mixed with the MNPs to give concentrations from 4 mg/ml to 32 mg/ml, and were placed in Petri dishes. Glass slides which had been pre-cleaned with piranha solution were placed at the base of the dishes, which were then transferred to a sealed desiccator containing solid ammonium carbonate (Sigma-Aldrich). Crystallization was then allowed to proceed for 1 day, after which time the glass slides were removed from solution, and were washed with water before being allowed to air dry.

Characterization of Calcium Carbonate Composite Crystals: The morphologies of the $CaCO_3$ particles and their association with the MNPs were determined using a range of analytical techniques including optical microscopy, scanning electron microscopy (SEM), transmission electron microscopy (TEM), Raman microscopy, thermogravimmetric analysis (TGA), powder X-ray diffraction (XRD) and atomic absorption spectroscopy (AAS). The morphologies of the crystals were determined using SEM, where the glass cover slip supporting the crystals was mounted on an SEM stub using an adhesive carbon pad, and samples were Pt/Pd coated, prior to viewing with a JEOL 6330 FEG-SEM operating at 10 kV. Characterisation of the crystal polymorph was carried out using Raman microscopy of individual particles, where Raman microscopy was performed using a Renishaw Raman 2000 System Microscope operating with a 785 nm laser. The MNPs were also confirmed to be magnetite using powder XRD, using a Bruker D8 Advance X-ray Diffractometer

Supplementary Information

The composite crystals were also examined to determine their composition, and to characterize the distribution of MNPs within the calcite single crystal. Atomic Absorption Spectroscopy (AAS) was used to determine the amounts of Fe and Ca in the crystals, where they were dissolved in 5 % nitric acid and analyzed using a Perkin-Elmer Atomic Absorption Spectrometer AAnalyst 400, operating with an air-acetylene flame. Thermogravimetric analysis also gave information on composition, and was carried out using a Netzsch STA 409 EP TGA, where samples were heated in air at a rate of 5 ^{o}C min^{-1} over the temperature range 25 ^{o}C to 900 ^{o}C. The distribution of MNPs throughout the calcite single crystal lattice was investigated using TEM. Cross sections (lamellae) through the crystals were prepared by cutting the crystals using Focussed Ion Beam Milling (FIB), where this was carried out with a FEI FIB-201, operating at 30 keV with gallium ions. A lamella of size 10 × 5 micron was mounted on to a bar in the copper FIB lift-out grid, and was held in place during the FIB by depositing platinum over the end of the lamella resting on the grid bar, thereby welding it in place. TEM and EDXA were carried out using a FEI Tecnai TF20 FEG-TEM Field emission gun TEM/ STEM operating at 200 kV which was fitted with an HAADF detector, an Oxford Instruments INCA 350 EDX system/80mm X-Max SDD detector and a Gatan Orius SC600A CCD camera. Finally, the magnetic properties of the MNPs and the calcite/MNP composites were determined using an Oxford Instruments Vibrating Sample Magnetometer (VSM) at temperatures from 4 K to room temperature, with a sensitivity of 5 μemu.

Supplementary Information

Table S1. Summary of the morphologies of the calcium carbonate crystals precipitated after 1 day in the presence of magnetite nanoparticles functionalized with $PMAA_{23}$-$PStSNa_{200}$. Representative images of the different morphological types are shown in Figure S5.

	Concentration of MNPs (mg/ml)					
[Ca^{2+}]		**0.1**	**0.4**	**4.0**	**10.0**	**20.0**
	1.5 mM	Rhombohedral	Rhombohedral	Mesocrystals	A few mesocrystals	No crystals
	3 mM	Rhombohedral	Mesocrystals	Mesocrystals	A few mesocrystals	No crystals
	6 mM	Rhombohedral	Intergrown	Polycrystals		
	10 mM	Intergrown	Intergrown	Flower-like		
	20 mM	Intergrown	Polycrystals	Flower-like		

Supplementary Information

Figure S1. (a) Transmission electron micrograph of magnetite nanoparticles coated with $PMAA_{23}$-$PStSNa_{200}$, showing an average particle diameter of ≈ 8nm. (b) A powder XRD spectrum of the particles confirming that they are magnetite.

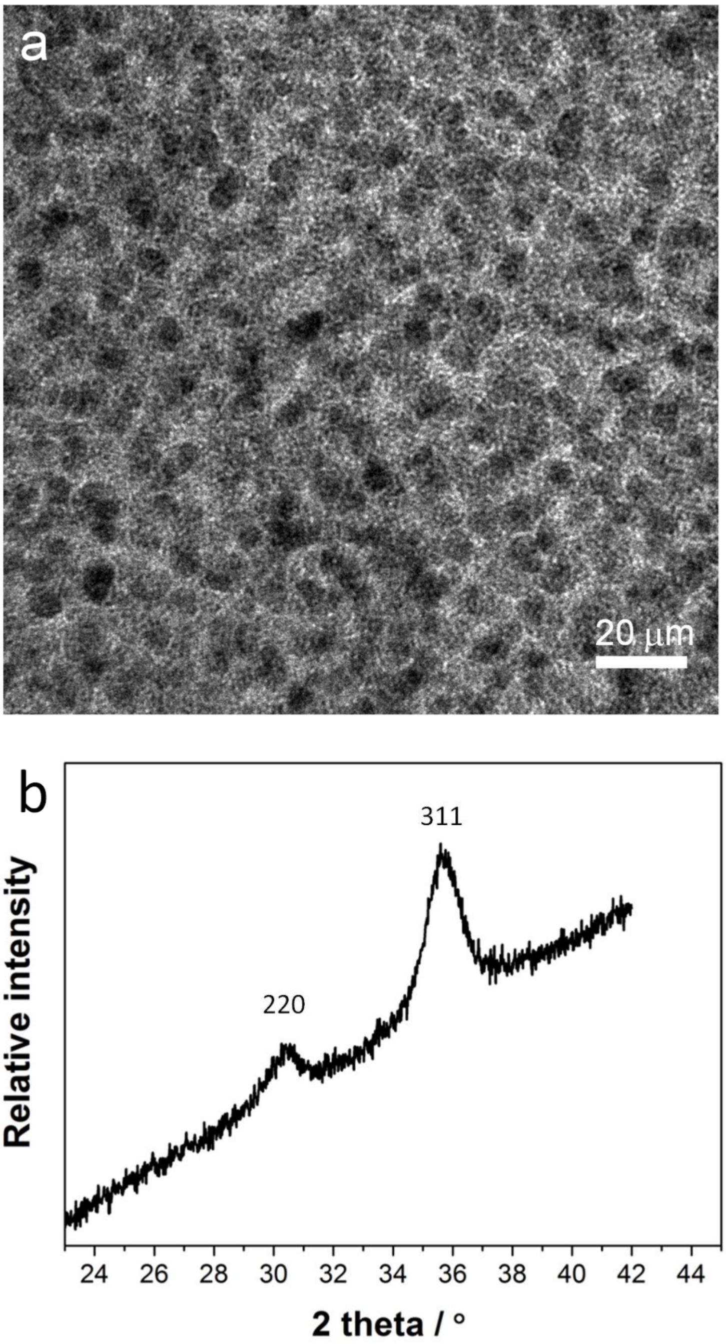

Supplementary Information

Figure S2. Thermogravimetric analysis (TGA) of magnetite nanoparticles coated with $PMAA_{23}$-$PStSNa_{200}$, demonstrating that they comprise approximately 50 wt% copolymer.

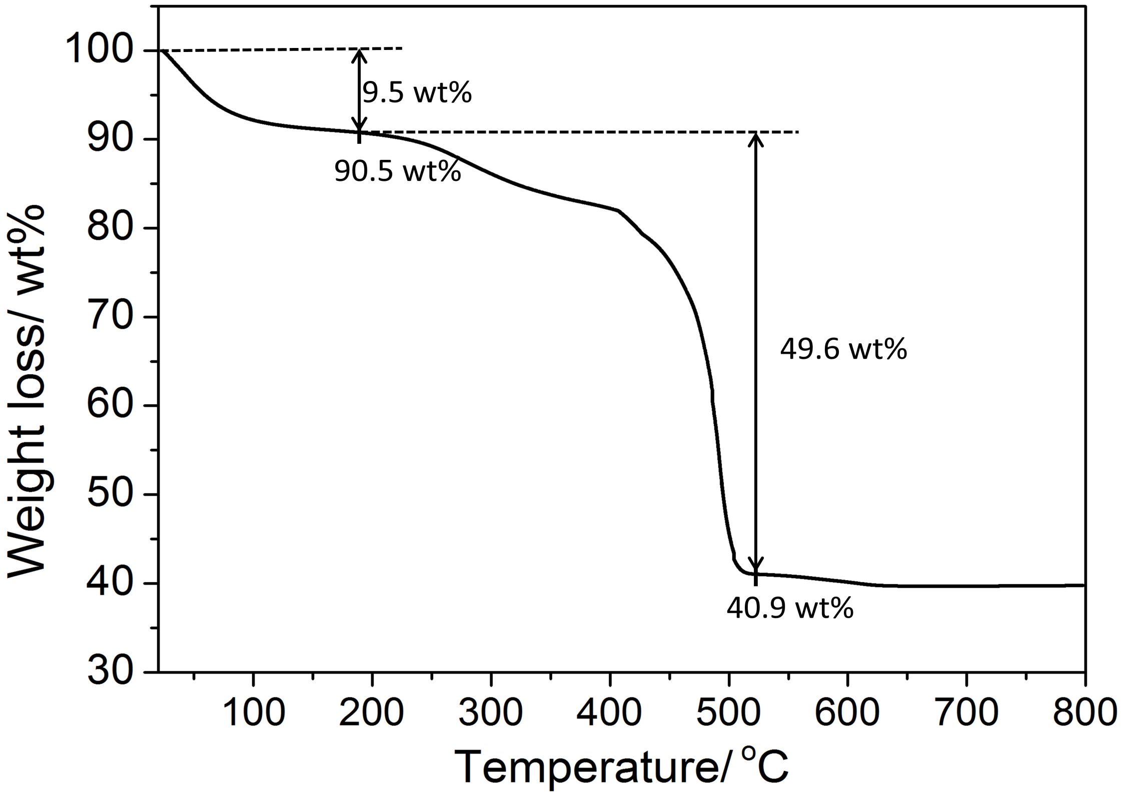

Figure S3. Calcite rhombohedra precipitated (a) in the absence of nanoparticle additives, and (b) in the presence of uncoated magnetite nanoparticles.

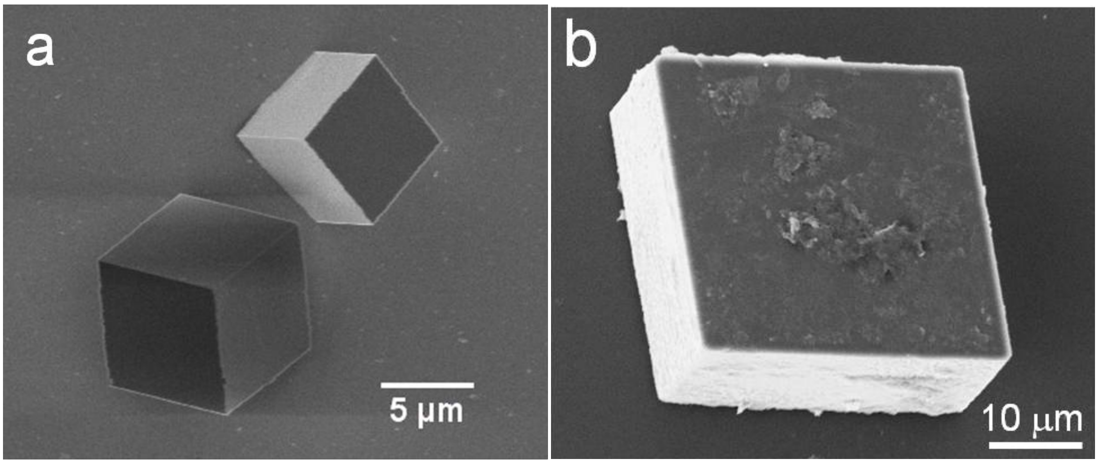

Supplementary Information

Figure S4. $CaCO_3$ particles precipitated in the presence of copolymer-coated MNPs. (a) Rhombohedral calcite produced at $[Ca^{2+}]$ = 1.5 M and [MNP] = 0.1 mg/ml, (b) Calcite with "mesocrystal" morphology produced at $[Ca^{2+}]$ = 3 mM and [MNP] = 0.4 mg/ml; (c) Intergrown calcite particle produced at $[Ca^{2+}]$ = 10 mM and [MNP] = 0.10 mg/ml; (d) "Polycrystalline calcite produced at $[Ca^{2+}]$ = 20 mM and [MNP] = 0.10 mg/ml and (e) flower-like calcite produced at $[Ca^{2+}]$ = 10 mM and [MNP] = 0.4 mg/ml.

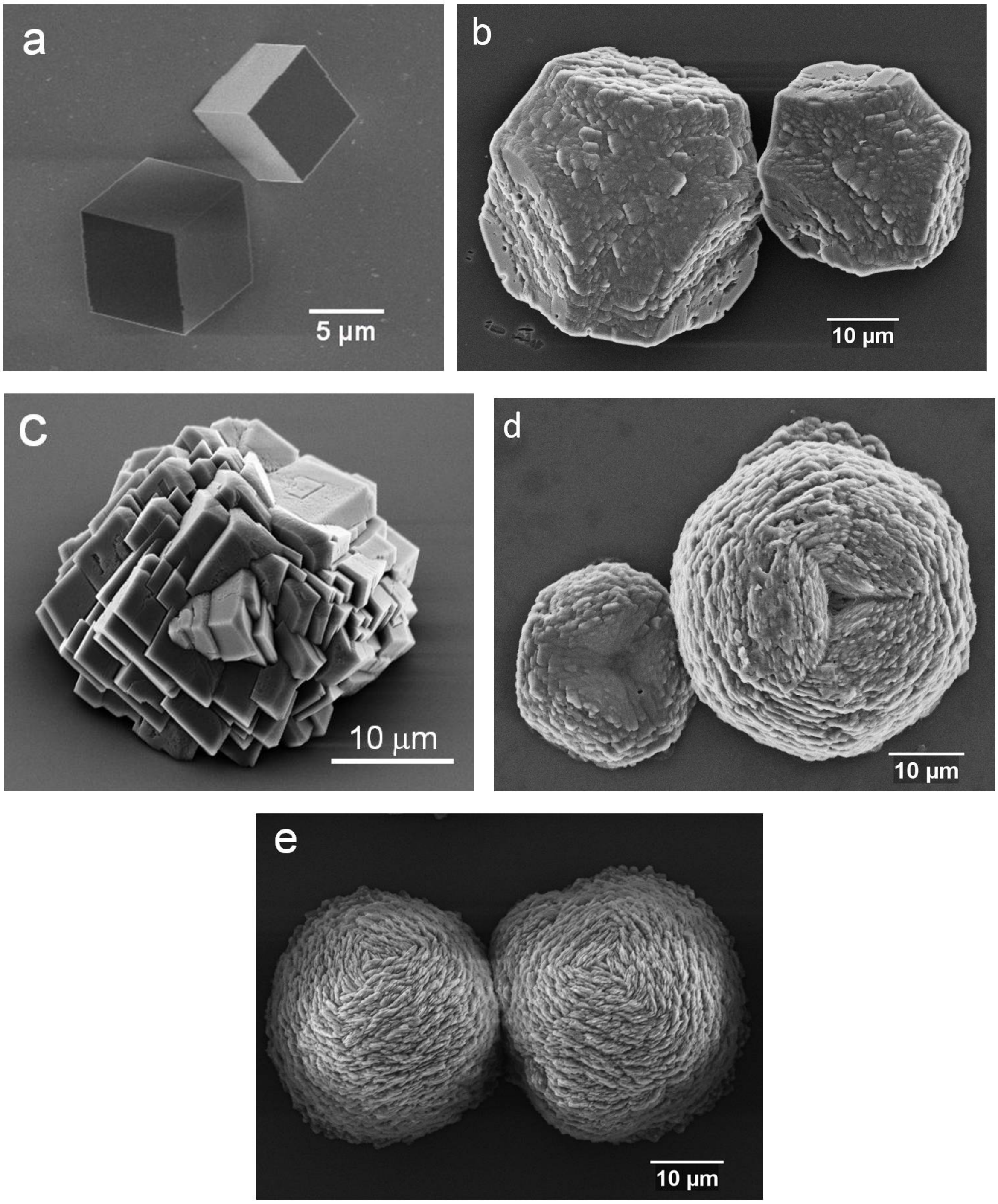

Supplementary Information

Figure S5. (a) EDX spectrum of the cross-section through a calcite single crystal containing copolymer-stabilized MNPs, showing the presence of Fe and S. (b) Electron diffraction pattern taken from a thin section cut through the nanocomposite crystals, obtained by tilting the crystal off the diffraction angle of calcite. Rings corresponding to magnetite are observed together with a number of reflections from the calcite single crystal.

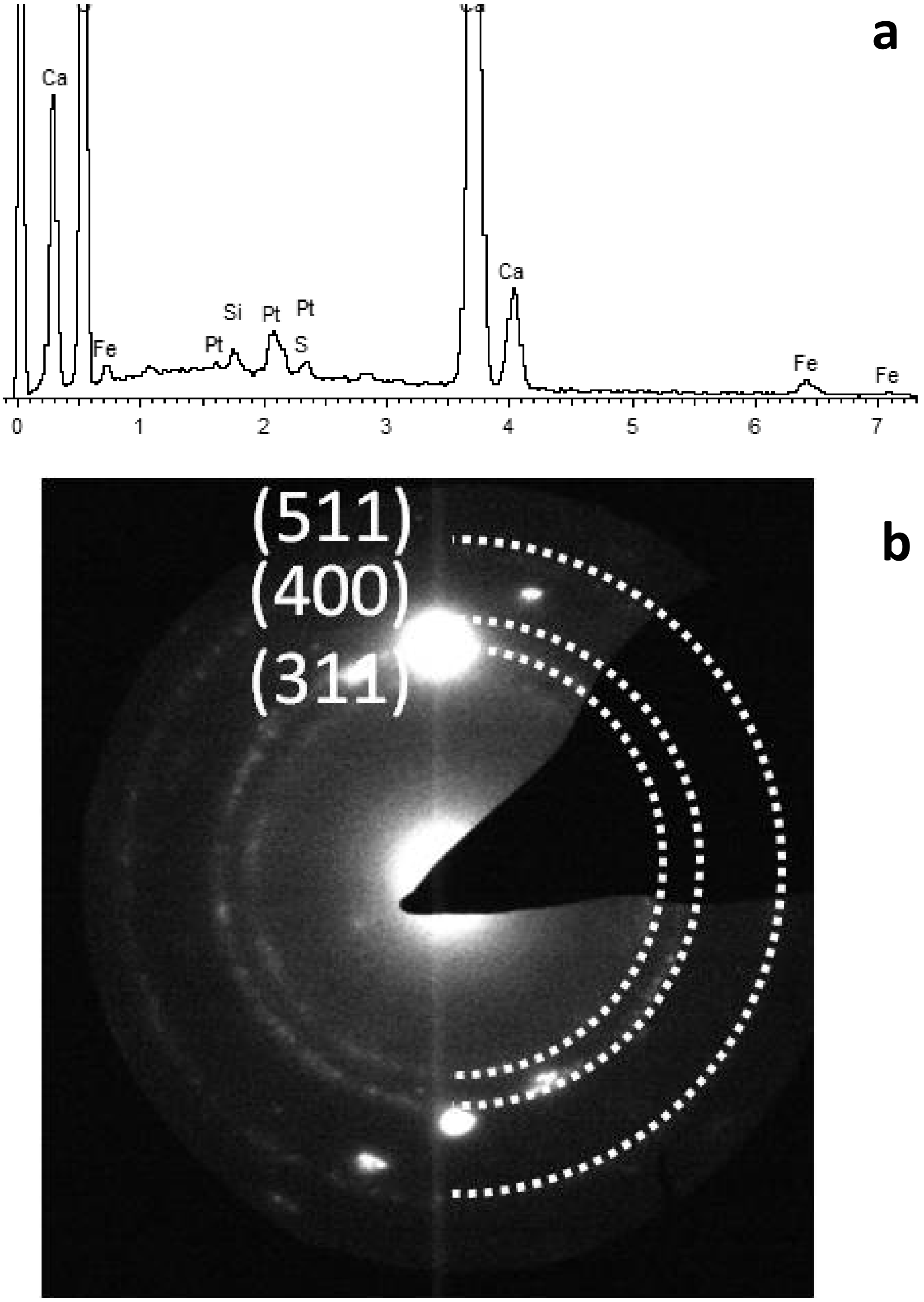

Figure S6. SEM image of a calcite nanocomposite crystal showing the area from which a lamella was cut by FIB for TEM imaging. (b) The section generated by FIB.

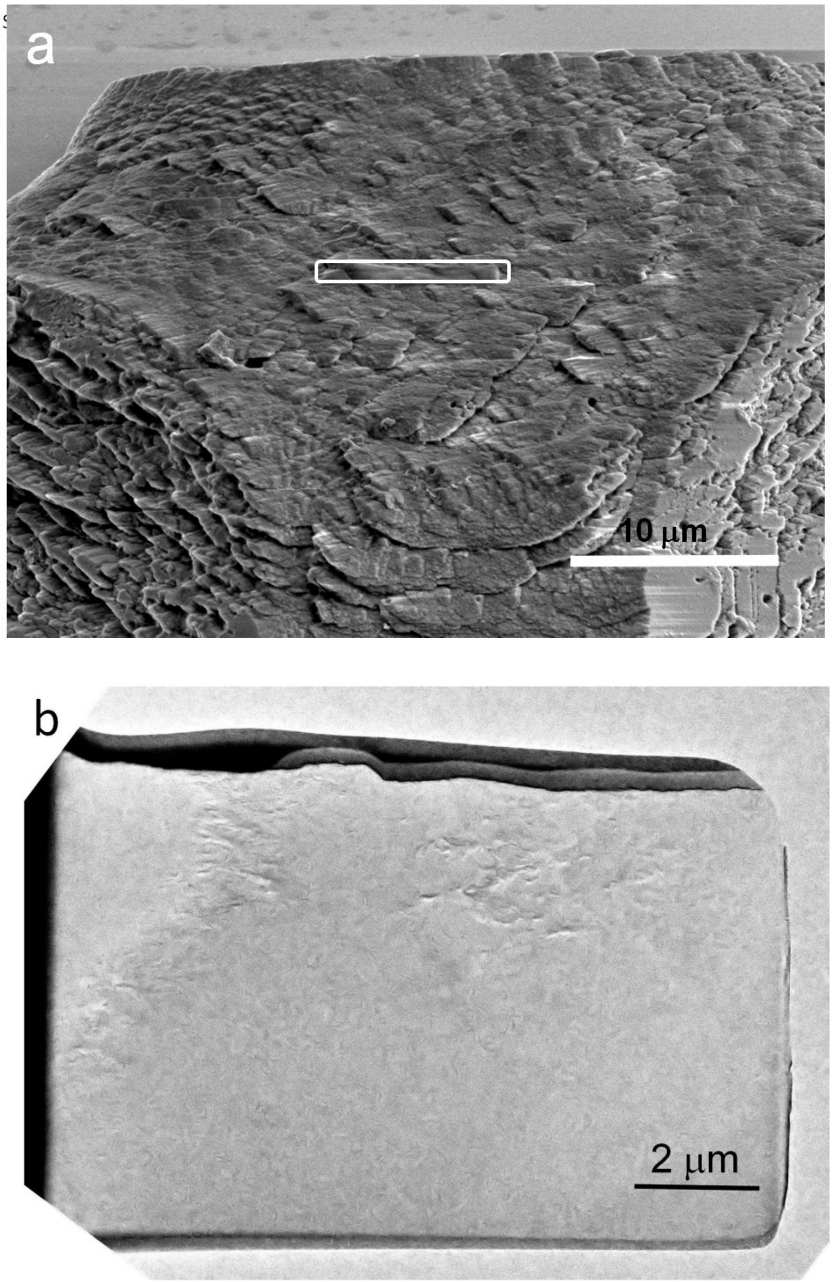

Figure S7. Thermogravimetric analysis (TGA) of calcite crystals containing copolymer-stabilized magnetite nanoparticles.

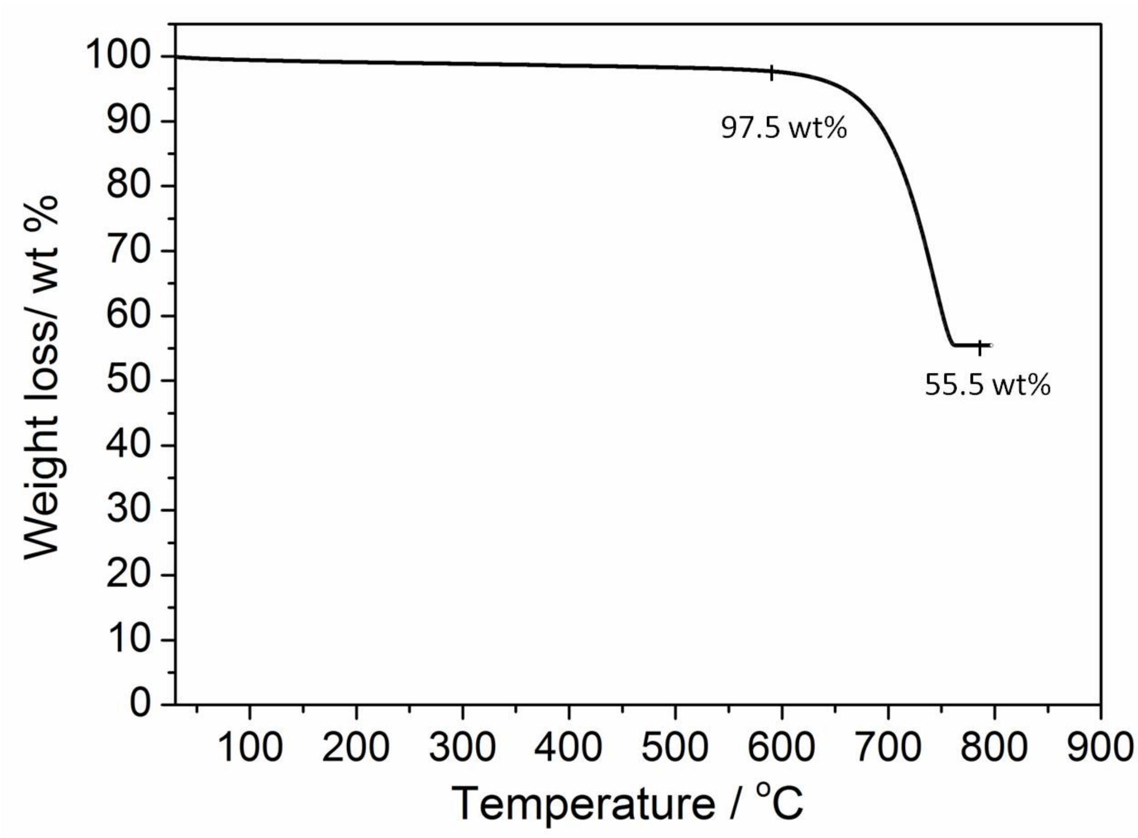

Analysis shows that the samples underwent a 2.5 wt% loss up to 550 °C, which can be attributed to copolymer pyrolysis products and water (1.2 wt%), and a further 42 wt% loss above 600 °C, leaving final residues of 55.5 wt% at 800 °C. As we have shown in previous work, entrapment of organic additives within single crystals of calcite inhibits their release from the crystal on annealing.[5] Therefore, while annealing of pure copolymer results in its full decomposition below 550 °C, temperatures exceeding 600 °C cause oxidation of the magnetite to α-Fe_2O_3 (hematite), as well as decomposition of the calcium carbonate and any remaining copolymer residues. However, assuming that the original nanocomposite crystals contain 5.4 wt% of magnetite (as shown by atomic absorption) and that the copolymer decomposes completely, 5.6 wt% of the final residue of 55.5 wt% can be attributed to pure iron oxide particles, and 49.2 wt% to CaO. The 42 wt% loss above 600

^{o}C is then due to loss of 38.2 wt % CO_2 from stoichiometric decomposition of $CaCO_3$ (100 wt % $CaCO_3$ = 56 wt % CaO + 44 wt% CO_2), an increase of 0.2 wt% due to oxidation of 5.4 wt% Fe_3O_4 to Fe_2O_3 and loss of 4 wt% due to the decomposed copolymer. In combination with the 1.3 wt% of copolymer lost below 550 ^{o}C, this gives 5.3 wt % of copolymer in the original nanocomposite, which is in good agreement with the approximately 1:1 ratio of copolymer corona and iron oxide core of the stabilized MNPs.

References

(1) Semsarilar, M.; Ladmiral, V.; Blanazs, A.; Armes, S. P. *Langmuir* **2012**, *28*, 914.

(2) Couvreur, L.; Lefay, C.; Belleney, J.; Charleux, B.; Guerret, O.; Magnet, S. *Macromolecules* **2003**, *36*, 8260.

(3) Yuan, J. J.; Armes, S. P.; Takabayashi, Y.; Prassides, K.; Leite, C. A. P.; Galembeck, F.; Lewis, A. L. *Langmuir* **2006**, *22*, 10989.

(4) Ihli, J.; Bots, P.; Kulak, A.; Benning, L. G.; Meldrum, F. C. *Adv. Func. Mater.* **2013**, *23*, 1965.

(5) Kim, Y. Y.; Ganesan, K.; Yang, P.; Kulak, A. N.; Borukhin, S.; Pechook, S.; Ribeiro, L.; Kröger, R.; Eichhorn, S. J.; Armes, S. P.; Pokroy, B.; Meldrum, F. C. *Nature Mater.* **2011**, *10*, 890.